Articles

The Discovery of New 11β-Hydroxysteroid Dehydrogenase Type 1 Inhibitors by Common Feature Pharmacophore Modeling and Virtual Screening

Daniela Schuster,[†,‡] Evelyne M. Maurer,[‡,§] Christian Laggner,[†] Lyubomir G. Nashev,[§] Thomas Wilckens,[||] Thierry Langer,*[,†] and Alex Odermatt*[,§]

Institute of Pharmacy, Department of Pharmaceutical Chemistry, University of Innsbruck, Innrain 52c, and Center for Molecular Biosciences Innsbruck (CMBI), Peter Mair-Strasse 1a, 6020 Innsbruck, Austria, Department of Nephrology and Hypertension, Department of Clinical Research, University of Berne, Freiburgstrasse 15, 3010 Berne, Switzerland, and BioNetWorks GmbH, Jakob-Klar-Strasse 7, 80796 Munich, Germany

Received January 24, 2006

11β-Hydroxysteroid dehydrogenase (11β-HSD) enzymes catalyze the conversion of biologically inactive 11-ketosteroids into their active 11β-hydroxy derivatives and vice versa. Inhibition of 11β-HSD1 has considerable therapeutic potential for glucocorticoid-associated diseases including obesity, diabetes, wound healing, and muscle atrophy. Because inhibition of related enzymes such as 11β-HSD2 and 17β-HSDs causes sodium retention and hypertension or interferes with sex steroid hormone metabolism, respectively, highly selective 11β-HSD1 inhibitors are required for successful therapy. Here, we employed the software package Catalyst to develop ligand-based multifeature pharmacophore models for 11β-HSD1 inhibitors. Virtual screening experiments and subsequent in vitro evaluation of promising hits revealed several selective inhibitors. Efficient inhibition of recombinant human 11β-HSD1 in intact transfected cells as well as endogenous enzyme in mouse 3T3-L1 adipocytes and C2C12 myotubes was demonstrated for compound **27**, which was able to block subsequent cortisol-dependent activation of glucocorticoid receptors with only minor direct effects on the receptor itself. Our results suggest that inhibitor-based pharmacophore models for 11β-HSD1 in combination with suitable cell-based activity assays, including such for related enzymes, can be used for the identification of selective and potent inhibitors.

Introduction

Glucocorticoids are important regulators of various physiological processes including immunomodulation, cell growth, and energy metabolism.[1,2] Chronic glucocorticoid excess has been associated with many diseases including muscle wasting, osteoporosis, cataract formation, cognitive disorders, and the metabolic syndrome, which is characterized by several clinical features such as visceral obesity, insulin resistance, diabetes, hypertension, dyslipidemia, and atherosclerosis. Glucocorticoids antagonize the effects of insulin and leptin,[3,4] and they stimulate hepatic glucose production and reduce glucose uptake in adipose tissue and skeletal muscle;[5−8] therefore, chronically elevated glucocorticoid concentrations contribute to glucose intolerance.

In particular, enhanced local reactivation of glucocorticoids rather than systemically elevated glucocorticoid levels have been associated with metabolic disease.[9] Inactive 11-ketoglucocorticoids [cortisone (**1**) in humans and 11-dehydrocorticosterone in rodents] are converted to active 11β-hydroxyglucocorticoids [cortisol (**2**) in humans and corticosterone in rodents] by 11β-HSD1, an enzyme expressed ubiquitously that plays an essential role in the liver, adipose tissue, and skeletal muscle. Transgenic overexpression of 11β-HSD1 in adipose tissue in mice caused visceral obesity, glucose intolerance, and insulin resistance,[10,11] while overexpression in the liver caused metabolic syndrome without obesity.[12] In contrast, 11β-HSD1 knock-out animals were resistant to the development of high-fat diet-induced diabetes.[13] Investigations in humans provided evidence for enhanced expression of 11β-HSD1 in adipose tissue of obese patients and in skeletal muscle of diabetic patients, while its expression was found to be reduced in the liver.[6,14−18] Thus, 11β-HSD1, which is considered as a promising target for treatment of glucocorticoid-dependent disease, may exert various functions in different tissues, suggesting that inhibitors with distinct properties may be required for successful tissue-specific therapeutic applications.

A second enzyme, 11β-HSD2, catalyzes the reverse reaction, e.g., the inactivation of glucocorticoids, and is expressed mainly in kidney and placenta, where it protects mineralocorticoid receptors (MR) from activation by glucocorticoids.[19] Although 11β-HSD1 and 11β-HSD2 both catalyze the interconversion of glucocorticoids (Figure 1), they are functionally quite different,[20] have only 18% identical amino acid sequences, and share a higher similarity with other members of the short chain dehydrogenase/reductase (SDR) family.[21]

SDR enzymes share a conserved α/β nucleotide-binding Rossman fold consisting of five stranded parallel β-sheets flanked by three α-helices on the right and left side each. SDR reactions are catalyzed by a Tyr-$(Xaa)_3$-Lys motif, which is often combined with a conserved Ser that orients the substrate. The conserved Lys residue forms hydrogen bonds with the nico-

* To whom correspondence should be addressed. (A.O.) Tel: +41/31/632-9438. Fax: +41/31/632-9444. E-mail: alex.odermatt@dkf.unibe.ch. (T.L.) Tel: +43/512/507-5252. Fax: +43/512/507-2940. E-mail: Thierry.Langer@uibk.ac.at.

† University of Innsbruck.

‡ These authors contributed equally to the present work.

§ University of Berne.

|| BioNetWorks GmbH.

10.1021/jm0600794 CCC: $33.50
Published on Web 05/19/2006

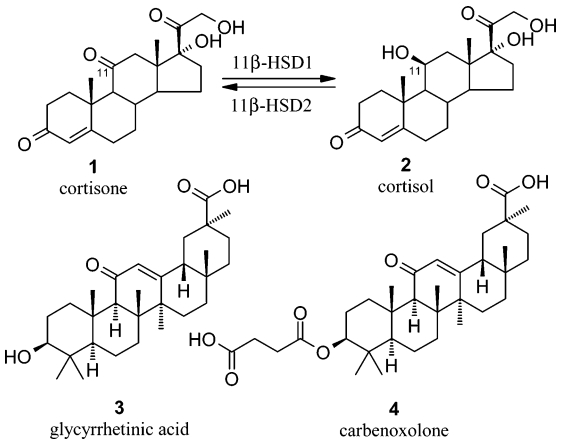

Figure 1. 11β-HSD enzymes catalyze the interconversion of cortisone and cortisol. Glycyrrhetinic acid (GA) and carbenoxolone (CBX) constitute prominent, nonselective 11β-HSD inhibitors.

tinamide ribose and lowers the pK_a of the Tyr hydroxyl group to promote proton transfer.[22]

With the recent elucidation of the murine, guinea pig, and human 11β-HSD1 X-ray crystal structures (PDB entry 2bel),[22−25] a valuable basis for the proper investigation of the enzyme's function and for rational inhibitor design is now available. 11β-HSD1 uses the cofactor NADPH to reduce **1** to **2**. In all three published human crystal structures, the cocrystallized ligand was observed in close vicinity to the cofactor molecule NADPH as well as the catalytic amino acid residue Tyr183. Ser170 participated in ligand binding, stabilizing the orientation within the active site.

As manual positioning and pharmacophore-based fitting of ligands into the binding pocket suggest, various steroids such as **1** and 7-ketocholesterol could bind in a perpendicular orientation relative to the observed position of CHAPS (PDB entries 1xu7 and 1xu9) and **4** (carbenoxolone, CBX, PDB entry 2bel).[22,25,26]

In recent years, molecular modeling has gained much importance in the field of drug discovery and development.[27−29] Various computational approaches are now available to complement the array of hit and lead discovery technologies, among which virtual screening (VS) is most popular. VS methods are designed for searching large compound databases in silico and selecting a limited number of candidate molecules for in vitro testing to identify novel chemical entities that have the desired biological activity.[30] VS can be applied to search for new active hits out of a virtual library that represents an existing compound library, and it can also be employed for an estimation of ADME parameters, drug-likeness, and toxicity.[27,28,31−34] In a comparison of hit rates from high throughput screening (HTS) and VS, Doman et al.[35] demonstrated the power of the VS approach. HTS of 400000 compounds resulted in 85 hits with IC_{50} values < 100 μM and six of them with IC_{50} values < 10 μM. Biological testing of 365 proposed compounds derived by molecular docking returned 127 hits with IC_{50} values < 100 μM of which 21 had IC_{50} values < 10 μM. This study showed that the modest HTS hit rate of 0.021% was dramatically outperformed by VS (hit rate of 34.8%).

At the beginning of our modeling studies, no X-ray crystal structure of 11β-HSD1 was available. Accordingly, we employed ligand-based pharmacophore models as VS tools for the identification of novel classes of 11β-HSD1 inhibitors. Because inhibition of renal 11β-HSD2 would result in **2**-dependent activation of MR, thereby causing sodium retention and hypertension, and inhibition of 17β-HSDs would interfere with local estrogen metabolism, the compounds selected from in silico screening were subjected to biological testing using several cell-based assays.

Chart 1. Training Set Compounds for the 11β-HSD1 Inhibitor Pharmacophore Model

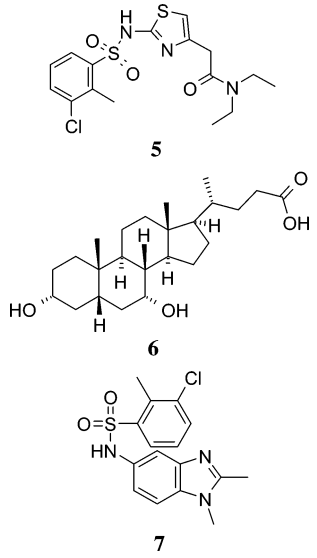

Results

Ligand-Based Pharmacophore Modeling for Selective 11β-HSD1 Inhibitors. Several preferably selective inhibitors of 11β-HSD1 are known from literature, many of them belonging to the structural class of arylsulfonamides.[36,37] The training set compounds were selected from the stockroom DB (a pool of 144 compounds with known activity on one or both 11β-HSD enzymes; see Supporting Information Table S-1) based on high activity, selectivity, and chemical diversity. As a training set for the 11β-HSD1 inhibitor pharmacophore model, the highly selective inhibitor **5** (CAS 376638-65-2),[36] **6** (chenodeoxycholic acid)—which preferentially inhibits 11β-HSD1[26,38,39]—and the potent 11β-HSD1 inhibitor **7** (CAS 686746-69-0) for which the selectivity toward 11β-HSD2 has not been determined[37] were selected (Chart 1). The hypothesis generation process returned 10 hypotheses of which all contained six features. The first hypothesis consisted of four hydrophobic (H) features, one hydrogen bond acceptor (HBA) feature, and one hydrogen bond donor (HBD) feature. All other nine hypotheses lacked the HBD feature; a second HBA was present instead. Generally, HBD features make a model more restrictive than HBA features, which results in less abundant hitlists when employing the pharmacophore model as a VS tool. Therefore, the first hypothesis was picked for further refinement. If a model contains no spatial restrictions, a VS run can return hits that are too spacious to fit into the ligand binding site. When employing ligand-based models, spatial information on known active ligands can be included by fitting active, large, and rigid compounds into the model and converting the molecule into a shape query. When the derived shape is merged with the initial hypothesis, compounds that stick out of this shape when fitted into the model will be excluded from the VS hitlist. As a spatial refinement for the 11β-HSD1 inhibitors model, the rigid compound **6** was fitted into the pharmacophore, converted into a shape query, and merged with the initial hypothesis (Figure 2). This extended model—"hypothesis 1"—was supposed to identify preferably 11β-HSD1 selective compounds.

To test the potential of hypothesis 1 to identify potent, selective 11β-HSD1 inhibitors, the so-called stockroom database

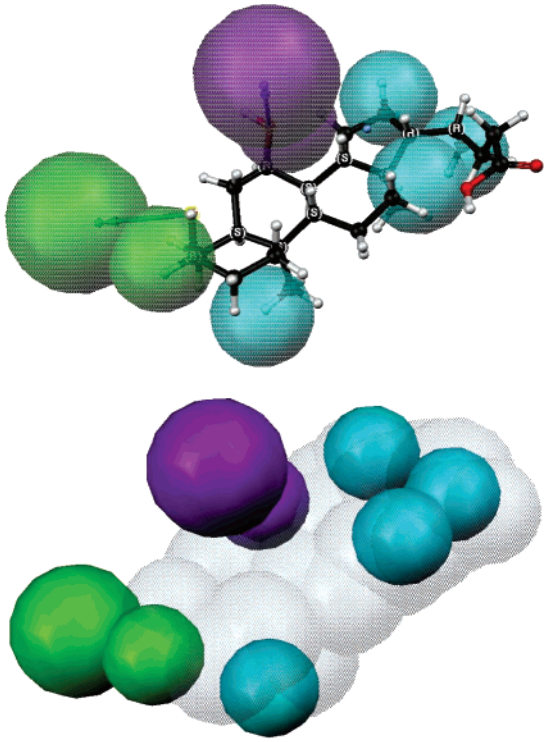

Figure 2. Compound **6** fitted into hypothesis 1 without shape. H features are shown in cyan, HBAs are shown in green, and HBDs are shown in violet (top). Hypothesis 1 without a fitted ligand. The shape of **6** is depicted in gray (bottom).

consisting of 144 11β-HSD inhibitors (Supporting Information Table S-1) with different potency and selectivity was searched using the Best Flexible Search algorithm. The search returned 17 hits including two compounds of the training set (Table 1). The other 15 hits comprised compounds with different (weak to potent) activity on 11β-HSD1. However, none of these hits was a known nonselective or a type 2 selective inhibitor. Conclusively, hypothesis 1 should return only hits with a satisfactory selectivity toward 11β-HSD2.

In addition to this first screening, the Derwent World Drug Index (WDI) database[40]—a database comprising 63307 compounds that are currently marketed as drugs or that are under clinical investigation—was searched with hypothesis 1 employing the Fast Flexible Search algorithm. With this second validation step, the promiscuity of the model was determined. A promiscuous model has a higher hit rate from a random druglike database (such as the WDI) than a specific one. This search returned 365 hits (0.6%) including some known active compounds, e.g., **6**. Taken altogether, hypothesis 1 was able to identify several 11β-HSD1 inhibitors out of the stockroom DB while excluding known selective 11β-HSD2 inhibitors from the hitlist. Furthermore, the random hit rate determined by a VS run in the WDI was low. Thus, this model should be suitable as a VS tool for new 11β-HSD1 inhibitors.

Ligand-Based Pharmacophore Modeling for Nonselective 11β-HSD Inhibitors. Currently, no selective and highly potent inhibitor of human 11β-HSD2 is known; thus, specific ligand-based pharmacophore modeling for this isoenzyme was not possible. Therefore, a nonselective model was developed as a VS tool for DB mining for 11β-HSD2 as well as 11β-HSD1 inhibitors. To retrieve a distinct model as compared to hypothesis 1, compounds that show preferable inhibition of 11β-HSD2 were selected for hypothesis generation. Only few data for such inhibitors are published; none of these compounds is highly selective. Recently, a potent and somehow selective inhibitor of rat 11β-HSD2 was reported. The 2-hydroxyethyl derivative of 18β-glycyrrhetinic acid (GA) amide inhibited 11β-HSD2 activity by 92% at a concentration of 10 μM, while 11β-HSD1 activity was only decreased by 36% under the same conditions. With an IC_{50} of 4 pM, this compound is the most potent and selective 11β-HSD2 inhibitor reported to date;[41] therefore, **23** (CAS 723294-42-6) was chosen as the first template structure for the nonselective pharmacophore model. Compound **4** is known as another potent inhibitor of 11β-HSD1 and 11β-HSD2. Published data from Barf et al. suggest that—although both 11β-HSD isoenzymes are potently inhibited by **4**—this compound inhibits human 11β-HSD1 with a 4-fold higher K_i value than human 11β-HSD2.[36] Therefore, **4** constitutes the second template structure for the new pharmacophore model (Chart 2). The pharmacophore generation process returned 10 hypotheses with 4−5 H features and four HBA features each. An evaluation by VS of the stockroom DB showed that the first hypothesis was most restrictive; therefore, it was refined by merging the shape of **23** with the model (Figure 3). The resulting pharmacophore—"hypothesis 2"—not only identified **23**, **4**, and two potent 11β-HSD inhibitors from the stockroom DB as actives, it also excluded known selective 11β-HSD1 inhibitors from the hitlist (Table 2).

To determine the random hit rate from a VS run in a druglike DB, the WDI was screened with hypothesis 2 employing the Fast Flexible Search algorithm, which returned eight hits (0.01%) including **4**. Accordingly, also, hypothesis 2 fulfilled the criteria for a suitable VS model.

Enrichment of Actives in a Random Druglike Database. In addition to the search in the Derwent WDI, which returned only 365 and eight "random" hits, respectively, we employed hypothesis 1 and hypothesis 2 in database searches in a virtual library described in ref 42. We seeded 10 active compounds—the GA analogues 18β-GA amide, **4**, **23**, **24**, and CAS 757218-99-8[55] as well as the bile acid **6** and the sulfonamides **7**, **8**, CAS 686746-46-3,[37] and CAS 686746-70-3[37]—into this DB and examined the enrichment of the hitlists.

Hypothesis 1 returned 136 hits (out of 12785 compounds, 0.08% of them actives); hypothesis 2 identified five compounds as hits from a best flexible search. Of the hits retrieved with hypothesis 1, two (1.5%) were known actives. All five compounds returned by a search with hypothesis 2 (100%) descended from our actives set. Taken together, seven of the 10 seeded actives were recovered by our two models. Five percent of our combined hitlist consisted of known actives, which corresponds to a 63-fold enrichment as compared to the initial virtual library.

Virtual Screening. DB mining of 12 commercially available compound libraries for new 11β-HSD1 and 11β-HSD2 inhibitors was conducted with hypothesis 1 and hypothesis 2 by using the Best Flexible Search algorithm of Catalyst (Table 3). Confronted with the abundance of hits derived by hypothesis 1, additional filter settings were used to select the most promising hits for biological testing. We did not employ Lipinskis rule of five for further filtering of the hitlist because many known potent 11β-HSD inhibitors do not meet the requirements of these rules. Many of them—e.g., **4**—have a molecular weight significantly greater than 500. So, the well-established rule of five might not be the best filter to discover highly active inhibitors for this target enzyme. Our custom filter included a Best Fit value $\geq$ 5, a maximum number of HBD features of five, a maximum number of HBA features of 10, no fitting into a hERG potassium channel block pharmacophore

Table 1. Hitlist Derived from a Stockroom DB Search with Hypothesis 1[a]

Compound	Reported Activity; BestFit	Compound	Reported Activity; BestFit
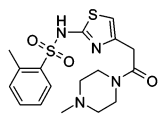 **8** BVT-2733	moderate, selective inhibitor of 11β-HSD1; BestFit: 5.6169	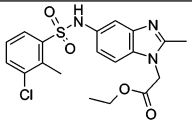 **9** CAS686746-86-1	moderate inhibitor of 11β-HSD1 (60), no data for 11β-HSD2; BestFit: 5.3613
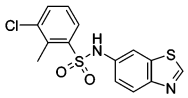 **10** CAS686746-63-4	weak inhibitor of 11β-HSD1 and 11β-HSD2 (4:10); BestFit: 4.0300	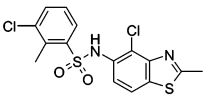 **11** CAS686746-82-7	moderate inhibitor of 11β-HSD1 (61), no data for 11β-HSD2; BestFit: 3.3197
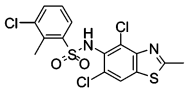 **12** CAS686746-87-2	moderate inhibitor of 11β-HSD1 (60), no data for 11β-HSD2; BestFit: 2.8926	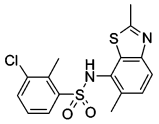 **13** CAS686746-91-8	moderate inhibitor of 11β-HSD1 (54), no data for 11β-HSD2; BestFit: 2.134
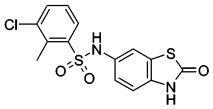 **14** CAS686746-66-7	weak inhibitor of 11β-HSD1 and 11β-HSD2 (8:2); BestFit: 1.9441	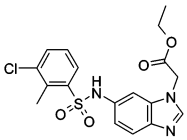 **15** CAS686746-84-9	moderate inhibitor of 11β-HSD1 (61), no data for 11β-HSD2; BestFit: 1.7273
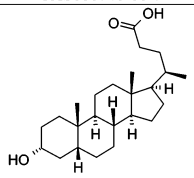 **16** lithocholic acid	potent inhibitor of 11β-HSD2, no data for 11β-HSD1; BestFit: 1.5821	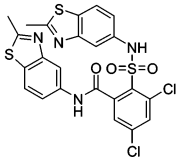 **17** CAS686746-41-8	moderate inhibitor of 11β-HSD1 and 11β-HSD2 (31:53); BestFit: 1.4807
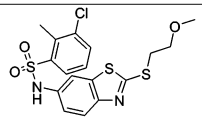 **18** CAS686746-67-8	weak inhibitor of 11β-HSD1 and 11β-HSD2 (20:6); BestFit: 1.2317	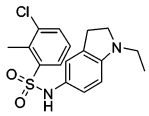 **19** CAS686747-50-2	moderate inhibitor of 11β-HSD1 (62), no data for 11β-HSD2; BestFit: 0.9954
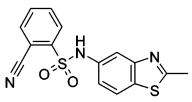 **20** CAS686746-48-5	weak, selective inhibitor of 11β-HSD1 (29); BestFit: 0.1521	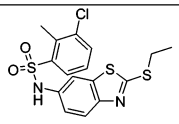 **21** CAS686746-64-5	weak inhibitor of 11β-HSD1 and 11β-HSD2 (10:5); BestFit: 0.1152
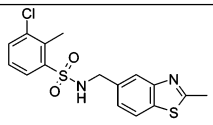 **22** CAS686746-72-5	moderate inhibitor of 11β-HSD1 (78), no data for 11β-HSD2; BestFit: 0.0799		

[a] Numbers in brackets indicate the % inhibition of the respective isoenzyme at a concentration of 10 μM. Compounds included in the training set of hypothesis 1 are excluded from this table.

model (which recognizes 80% of hERG channel blockers from a test set),[43] a cLogP of ≤ 5 indicating a low chance of bioavailability problems,[33] a calculated solubility of ≥ −5 (the computations of cLogP and solubility were performed with the

Chart 2. Training Set Compounds for the Nonselective Inhibitor Pharmacophore Model

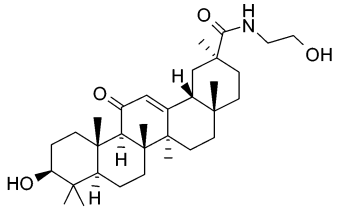

23

inhibition of 11β-HSD1: 11β-HSD2 = 1:3

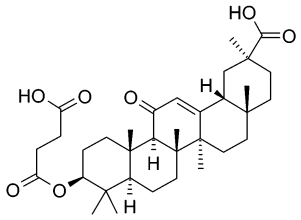

4

inhibition of 11β-HSD1: 11β-HSD2 = 1:4

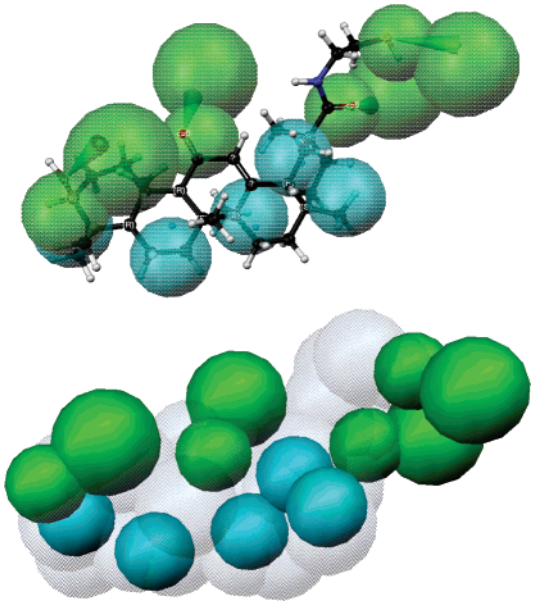

Figure 3. Compound **23** fitted into hypothesis 2 without shape (top). Nonselective pharmacophore model without a fitted ligand (bottom).

Osiris Property Explorer available at www.organic-chemistry-.org/prog/peo/index.html), and no structural relationship to already published sulfonamide derivatives.[37] Only 16 compounds of the preliminary 20304 hits met these stipulations. Of these 16 substances, 15 were available for purchase.

As listed in Table 3, out of the 1776579 compounds included in the DBs searched, only 107 (0.006%) compounds returned as hits from VS with hypothesis 2 (only hits with a Best Fit value > 0 were counted). From these 107 substances, 15 were chosen for biological testing. The compounds were selected based on chemical stability, Best Fit values, and availability.

In Vitro Validation of VS Hits. The VS protocol employed for searching inhibitors of 11β-HSD1 yielded 30 compounds that were then subjected to biological analysis for potential inhibition of human 11β-HSD1, 11β-HSD2, 17β-HSD1, and 17β-HSD2. The known, naturally occurring, and nonselective 11β-HSD inhibitor GA was used as a query compound. At a concentration of 10 μM, seven of the 30 compounds tested (compounds **25**−**31**; Chart 3 and Table 4) inhibited more than 70% of the activity of 11β-HSD1 when measured in cell lysates and were further investigated. None of the selected compounds showed any signs of toxicity at concentrations up to 40 μM in MTT cytotoxicity assays. As shown in Table 4, the IC_{50} values of all seven compounds were below 10 μM, with four compounds in the nanomolar range. The excellent fitting of **25**, **27**, and **31** into the respective hypotheses is shown in Figure 4.

To assess the selectivity of these compounds, inhibition of 11β-HSD2 was determined. Compounds **25** and **26**, which were predicted based on the 11β-HSD1-selective pharmacophore model, did not inhibit 11β-HSD2, whereas **27**−**31**, which were predicted based on the 11β-HSD unselective pharmacophore model, showed significant inhibition of 11β-HSD2 with IC_{50} values below 10 μM. Compound **27**, which has a sterol/steroid-like backbone, showed 27-fold preference to inhibit 11β-HSD1, whereas **28**−**31**, which have a GA- or **4**-like structure, inhibited 11β-HSD2 with a 3−4-fold preference. To further assess the specificity of the selected compounds, we determined their effect on the activities of 17β-HSD1 and 17β-HSD2 in cell lysates. Two compounds inhibited 17β-HSD1, but IC_{50} values were at least 10-fold higher than those for 11β-HSD1. Significant inhibition of 17β-HSD2 was observed for **26** and **30**, with IC_{50} values below 10 μM (Table 5).

A more reliable estimation of the potency of an inhibitor can be made in assays using intact cells. Therefore, we compared the potency of **25**−**31** in HEK-293 cells transiently expressing either 11β-HSD2 or 11β-HSD1 and hexose-6-phosphate dehydrogenase (H6PDH), which determines the reaction direction

Table 2. Hitlist Derived from a Stockroom DB Search with Hypothesis 2[a]

Compound	Reported Activity	Compound	Reported Activity
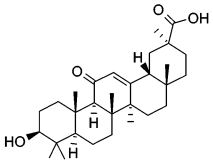 **3**	potent inhibitor of both 11β-HSD isoforms; BestFit: 1.27	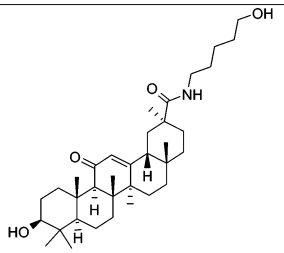 **24** XDS-01039	potent inhibitor of both 11β-HSD isoforms; BestFit: 1.42

[a] Compounds included in the training set of hypothesis 2 are excluded from this table.

Table 3. VS for 11β-HSD Inhibitors with Hypothesis 1 and Hypothesis 2

DB	DB size	no. of hits with best fit values > 0/% hits	
		hypothesis 1	hypothesis 2
Asinex Gold	199483	2667/1.3	4/0.002
Asinex Platinum	113364	2100/1.9	4/0.004
Bionet 2003	37826	265/0.7	0/0
ChemBridge DVS	29991	174/0.6	0/0
ChemDiverse Clab	202446	1459/0.7	14/0.007
ChemDiverse IDC	123000	1218/1.0	6/0.004
Enamine 03	300509	3875/1.3	32/0.011
Interbioscreen 03 nat	29977	484/1.6	25/0.083
Interbioscreen 03 syn	287726	3448/1.2	6/0.002
Maybridge 2003	59194	635/1.1	1/0.002
NCI	123219	446/0.4	4/0.003
Specs 09 03	269844	3533/1.3	11/0.004
total	1776579	20304/1.1	107/0.006

Table 4. Computed Properties for Compounds **1**−**7**[a]

compound	molecular weight	best fit value	cLogP	LogS
25	373.45	5.09, model 1	2.06	−3.22
26	450.32	5.08, model 1	3.3	−4.47
27	486.65	4.05, model 2	ND	ND
28	604.83	6.28, model 2	ND	ND
29	631.89	4.15, model 2	ND	ND
30	512.73	4.11, model 2	ND	ND
31	469.71	3.81, model 2	ND	ND

[a] ND, not determined.

of 11β-HSD1 as an oxoreductase and reflects the endogenous situation in metabolically relevant tissues[44−46] (Table 4). Although the query compound GA inhibited 11β-HSD2 with a 10-fold preference over 11β-HSD1 when measured in cell lysates, it inhibited both enzymes in intact cells showing a slight preference to inhibit 11β-HSD1. A similar observation was made with the GA derivatives **28**−**31**, which all showed a switch in their preference to inhibit 11β-HSD1 in intact cells. Because **25** and **27** displayed 10-fold selectivity to inhibit 11β-HSD1 in lysates and intact transfected HEK-293 cells, they were further tested in endogenous cell models.

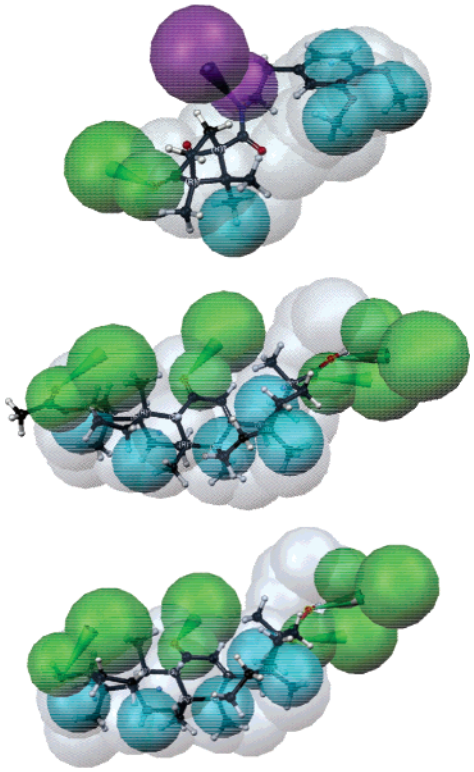

Figure 4. Compound **25** fitted into hypothesis 1 (top) and **27** (middle) and **31** (bottom) fitted into hypothesis 2.

Enhanced expression of 11β-HSD1 was found in myotubes from diabetic patients;[6] however, a suitable muscle cell-based assay allowing a more efficient analysis of inhibitors was not available. Here, we show that differentiated mouse C2C12 myotubes express 11β-HSD1 and efficiently catalyze the oxoreduction of **1** to **2**, comparable with the activity reported in differentiated mouse 3T3-L1 adipocytes.[44,47]

Analysis by quantitative real-time reverse transcriptase polymerase chain reaction revealed that both cell lines have very

Chart 3. Compounds **25**−**31** Derived from VS with Hypothesis 1 and Hypothesis 2

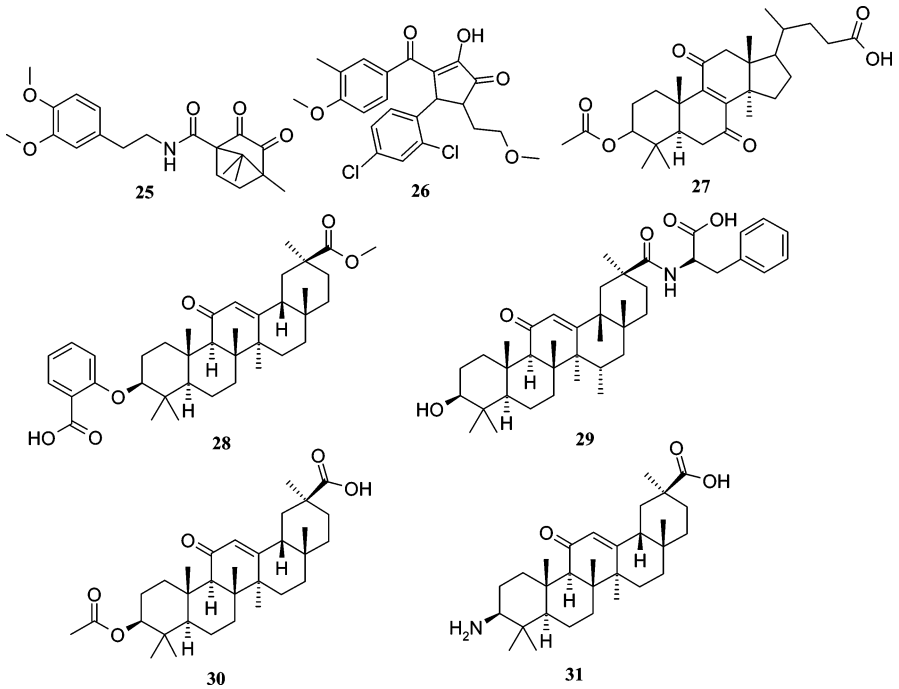

Table 5. Biological Activities of Selected Compounds Determined in Lysates of HEK-293 Cells Expressing Recombinant Enzymes or in Intact Transfected HEK-293 Cells[a]

no.	derived by hypothesis	IC_{50} (μM)					
		11βHSD1[b]	11βHSD2[b]	17βHSD1[b]	17βHSD2[b]	11βHSD1[c]	11βHSD2[c]
25	hypothesis 1	2.03 ± 0.18	ND[d]	20.2 ± 2.2	ND[d]	5.21 ± 0.68	ND[e]
26	hypothesis 1	7.59 ± 0.65	>30	>30	7.44 ± 1.10	>50	ND[e]
27	hypothesis 2	0.144 ± 0.027	3.95 ± 0.12	ND[d]	28.3 ± 5.5	0.41 ± 0.08	ND[e]
28	hypothesis 2	0.69 ± 0.06	0.28 ± 0.03	ND[d]	10.3 ± 1.3	3.84 ± 0.79	48 ± 16
29	hypothesis 2	2.81 ± 0.26	2.35 ± 0.48	>30	23.6 ± 6.4	12.6 ± 1.5	ND[e]
30	hypothesis 2	0.80 ± 0.09	0.201 ± 0.049	18.8 ± 7.3	3.78 ± 1.06	3.45 ± 0.47	6.43 ± 1.19
31	hypothesis 2	0.172 ± 0.031	0.060 ± 0.007	>30	ND[d]	1.02 ± 0.12	6.04 ± 0.84

[a] IC_{50} values were calculated by nonlinear regression analysis of the data from four independent experiments and represent means ± SD. [b] Determined in lysates of HEK-293 cells expressing recombinant enzymes. [c] Determined in intact transfected HEK-293 cells. [d] ND, inhibition not detectable at 30 μM. [e] Inhibition not detectable at 50 μM.

low levels of 11β-HSD1 in the undifferentiated state (C_t values of 29.5 for C2C12 and 29.4 for 3T3-L1, no conversion detectable after a 4 h incubation) but relatively high levels after differentiation (C_t values of 19.1 for C2C12 and 20.5 for 3T3-L1). H6PDH expression, which is essential for 11β-HSD1 oxoreductase activity,[44−46] does not significantly change during differentiation in both cell lines (C_t values of 23.3 and 22.7 for undifferentiated and differentiated C2C12 and 23.9 and 23.7 for undifferentiated and differentiated 3T3-L1 cells). Thus, differentiated C2C12 myotubes are a suitable cell system to study 11β-HSD1-mediated effects. As observed in HEK-293 cells transfected with both 11β-HSD1 and H6PDH, **27** efficiently inhibited conversion of **1** to **2**, with IC_{50} values of 0.33 ± 0.04 and 0.65 ± 0.08 μM in C2C12 myotubes and 3T3-L1 adipocytes, respectively. Compound **25** inhibited the 11β-HSD1-dependent conversion of **1** with IC_{50} values of 4.17 ± 0.91 and 3.90 ± 0.75 μM in C2C12 myotubes and 3T3-L1 adipocytes, respectively (Figure 5).

A potentially useful 11β-HSD1 inhibitor should block the local generation of **2** and reduce activation of glucocorticoid receptors (GR). Therefore, we assessed the cellular activity of **27** by performing a transactivation assay. The transcriptional activation of a galactosidase reporter gene under the control of a promoter containing a glucocorticoid response element was determined in HEK-293 cells transfected with GR, 11β-HSD1, and H6PDH. Addition of 250 nM **1** induced an approximately 30-fold increase of the galactosidase activity (positive control; Figure 6A). That this stimulation of transactivation is dependent on GR and 11β-HSD1 was verified by treatment of the cells with the GR antagonist RU486 and the nonspecific 11β-HSD1 inhibitor GA, which significantly reduced transcription of the galactosidase reporter gene. GR-dependent transactivation was then measured in cells treated with increased concentrations of **27**, and a dose-dependent inhibition was observed, with an IC_{50} of 2.09 ± 0.31 μM. As a control, HEK-293 cells were transfected with GR in the absence of 11β-HSD1 and H6PDH (Figure 6B). Whereas **1** did not affect transactivation, incubation of cells with 100 nM **2** induced transactivation approximately 60-fold. Compound **27** exerted a weak antagonistic effect, with an IC_{50} of transactivation observed at 11.8 ± 2.4 μM, suggesting that the antiglucocorticoid effect of **27** is mainly due to inhibition of 11β-HSD1-dependent reduction of **1** to **2**. As an additional control, we assessed the effects of **27** on MR (Figure 6C). Treatment with **1**, which does not bind to MR, had no effect on reporter gene expression, whereas **2** (not shown) and aldosterone strongly stimulated transactivation. Compound **27** exerted a weak antagonistic effect on MR, with an IC_{50} of 21 ± 4 μM. Thus, the antagonistic effect on both GR and MR occurs at 6−10-fold higher concentrations than the inhibition of 11β-HSD1.

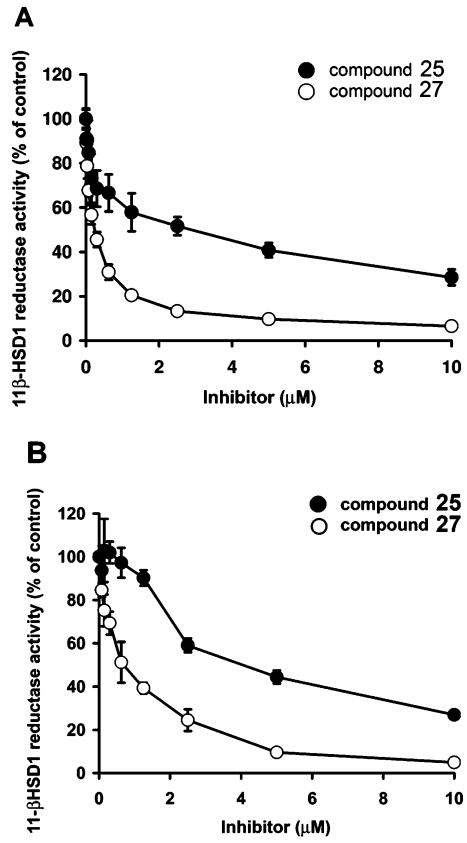

Figure 5. Inhibition of 11β-HSD1-dependent cortisone conversion in mouse C2C12 myotubes and 3T3-L1 adipocytes. The 11β-HSD1-dependent oxoreduction of 200 nM cortisone to cortisol in the presence of various concentrations of inhibitors was measured in fully differentiated mouse C2C12 myotubes (A) and in mouse 3T3-L1 adipocytes (B). Data represent means ± SD from four independent experiments and are expressed as the percentage of baseline activity in the absence of inhibitor. Filled circles, compound **25**; open circles, compound **27**.

Docking of New 11β-HSD1 Inhibitors. During the course of these studies, the X-ray crystal structure of human 11β-HSD1 has been published. To rationalize the potent inhibition of **25**, **27**, and **31**, they were docked into the ligand binding pocket (PDB entry 2bel). All three compounds occupied a similar but somewhat smaller area as compared to the observed binding position of **4** (Figure 7). All three docked structures formed interactions with the catalytically active amino acid residue Tyr183 in their best-ranked position: The amide nitrogen of **25** forms a hydrogen bond, and **27** and **31** have hydrophobic contacts with the aromatic part of Tyr183. In the 7th-best ranked solution of **27**, the keto oxygen at position 11 of the steroidal core is observed to hydrogen bond with Tyr183 as well (not depicted).

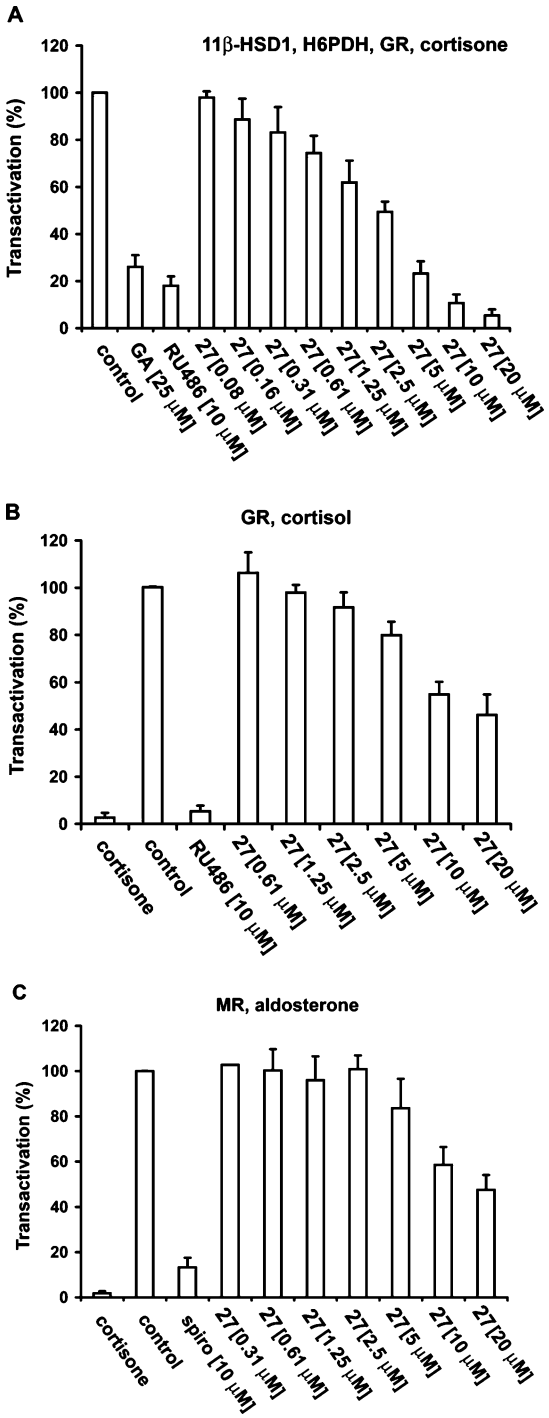

Figure 6. Inhibition of 11β-HSD1-dependent stimulation of GR-mediated transactivation by compound **27**. To assess 11β-HSD1-dependent activation of GR, HEK-293 cells transiently expressing pMMTV-LacZ, pCMV-LUC, and GR, 11β-HSD1, and H6PDH were incubated with 250 nM cortisone in the presence or absence of GR antagonist RU486, the known 11β-HSD inhibitor GA, or various concentrations of **27** (A). As a control to verify that the effect of **27** is primarily due to the inhibition of 11β-HSD1 and not to direct receptor antagonism, cells expressing pMMTV-LacZ, pCMV-LUC, and GR (B) or MR (C) were incubated with 100 nM cortisol (B) or 1 nM aldosterone (C) and various concentrations of **27**. After incubation for 24 h, galactosidase reporter activity, normalized to the internal luciferase control, was determined. Data (means ± SD from four independent experiments) represent the percentage relative to the control in the presence of the steroid but absence of inhibitor.

Comparison of the Ligand-Based Pharmacophore Models with the X-ray Crystal Structure of 11β-HSD1. When comparing the hydrogen bonding feature distances of hypothesis 1 with the arrangement of hydrogen bonds in the crystal structure, a good correlation of the distance between the ligand-based model and the crystal structure conformation could be observed. While the HBA and HBD features in hypothesis 1 are located 6.41 Å away from each other, a distance of 6.21 Å is found between the carboxyl group oxygen interacting with the Tyr183/ribose oxygen of NADPH (a bifurcated hydrogen bond) and the carbonyl oxygen interacting with the Ala172 backbone nitrogen (the only hydrogen bonds that **4** forms with 11β-HSD1 in the active site itself). Accordingly, the HBA feature of hypothesis 1 would represent the interaction of the ligand with the catalytically active Tyr183. The rest of the model is dominated by hydrophobic groups corresponding well to the predominantly hydrophobic character of the binding pocket. As hypothesis 2 was derived from relatively rigid GA derivatives including **4**, the structure-based model based on **4** revealed a high similarity, unsurprisingly.

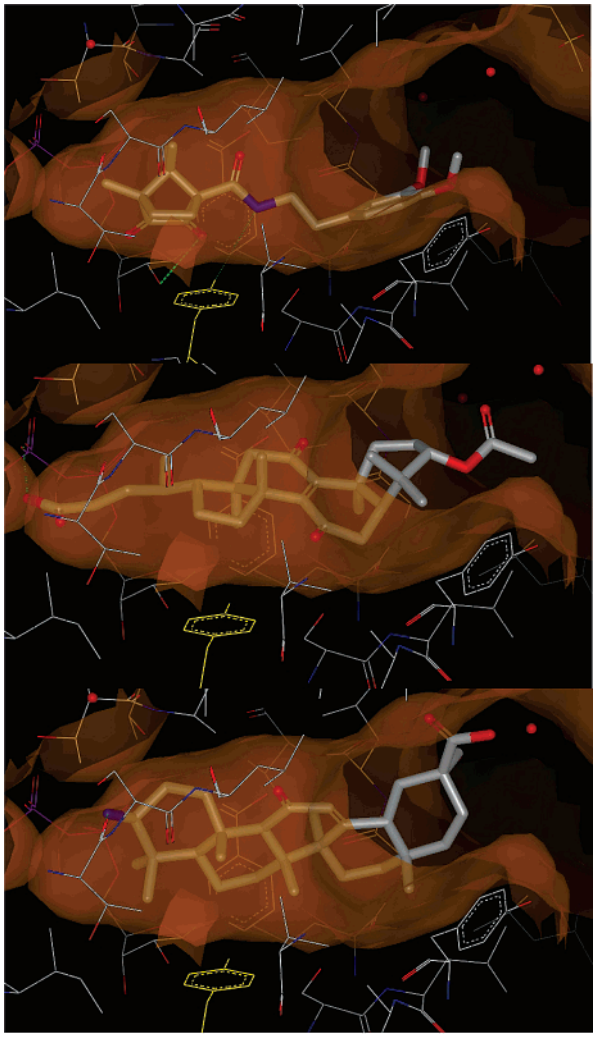

Figure 7. Docked positions of **25** (above), **27** (middle), and **31** (below) in the 11β-HSD1 ligand binding domain derived from the PDB entry 2bel. The binding pocket is colored orange, and the catalytically active residue Tyr183 is depicted in yellow.

Discussion

On the basis of recent experiments with transgenic animal models and observations in humans, an enhanced 11β-HSD1-dependent generation of active glucocorticoids in metabolically relevant tissues, such as liver, adipose tissue, and skeletal

muscle, is associated with visceral obesity, hyperglycemia, insulin resistance, and type 2 diabetes.[4,6,7,10,11,14−18] Thus, there is a great interest in the discovery of 11β-HSD1 inhibitors for the development of therapeutic interventions in metabolic syndrome but also for other glucocorticoid-dependent diseases such as impaired cognitive function,[48] wound healing,[49] and muscle atrophy. Indeed, arylsulfonamides and adamantly group containing inhibitors of 11β-HSD1 ameliorated several features of the metabolic syndrome and prevented progression of atherosclerosis in mice.[36,50−52] It can be anticipated that inhibition of 11β-HSD1 for distinct therapeutic applications will require compounds with different properties and tissue-specific distributions. Thus, there is a profound interest for the identification of novel classes of 11β-HSD1 inhibitors.

Several compounds inhibiting 11β-HSD1 but not 11β-HSD2, including the arylsulfonamides and adamantyl compounds, were discovered by HTS[36,52−54] or were derived from the known nonselective 11β-HSD inhibitor GA.[55] Here, as an alternative approach, we employed pharmacophore modeling and VS to identify novel 11β-HSD1 inhibitors.

In this study, the first pharmacophore models for 11β-HSD1 inhibitors are introduced. The hydrophobic core of the molecule corresponds to the sterol/GA-like part of many molecules that are substrates or inhibitors of 11β-HSD1. Steroidal structures are very common among endogenous and exogenous bioactive compounds. Selectivity of these compounds can be achieved via specific substitution patterns leading to hydrogen bonding networks, additional hydrophobic, or ionic interactions with the enzyme. In the case of 11β-HSD1, several amino acid residues of the binding pocket offer potential hydrogen bonding possibilities. In structure-guided approaches, one can consider whether a hydrogen bonding donor/acceptor group of a ligand is directly involved in ligand binding or not. However, in a ligand-guided approach, all hydrogen bonding groups have to be considered as putative essential interaction groups. Thus, a ligand-based pharmacophore model may contain more hydrogen bonding features than are required for ligand binding—as might be the case with hypothesis 2.

Both pharmacophore models constitute valuable tools in the search for new 11β-HSD1 inhibitors. Forty percent of the hits derived by the models showed over 50% 11β-HSD1 inhibition when tested at a concentration of 10 μM. While hypothesis 1 returned numerous hits from DB searches, which required additional filtering, hypothesis 2 was very restrictive. However, hits derived by hypothesis 1 preferably inhibited 11β-HSD1 in vitro while compounds selected by hypothesis 2 showed nonselective inhibition. Remarkably, our test compounds showed essentially similar inhibition profiles toward 11β-HSD1 and -2 as compared with the training set compounds.

When comparing the VS hits with the in vitro selectivity of the test compounds, the question arises why **27** was not derived by hypothesis 1. Fitting experiments with **27** revealed that the compound maps the chemical features of hypothesis 1 well—with the exception of the HBD feature. Compound **27** does not even have a HBD group as a substituent to the steroidal core. Accordingly, it can never return from a DB search with hypothesis 1 as a search query.

For lead compound identification, hypothesis 1 revealed more chemical diversity among biologically active hits than hypothesis 2, where mostly steroidal and GA-like compounds inhibited 11β-HSDs.

The selectivity of 11β-HSD1 inhibitors is usually assessed by testing such compounds for cross-inhibition of 11β-HSD2.[36,52−54] Inhibition of this enzyme in the kidney would result in **2**-induced activation of MR and cause hypertension.[19] Because both 11β-HSD1 and 11β-HSD2 catalyze the interconversion of glucocorticoids, 11β-HSD2 is intuitively chosen to assess the specificity of 11β-HSD1 inhibitors. However, a comparison of their amino acid sequences reveals that 11β-HSD1 and 11β-HSD2 are relatively distant enzymes, sharing only 18% identical sequences. In addition, 11β-HSD1 is facing the ER-lumen while 11β-HSD2 is oriented to the cytoplasm.[20,56] A phylogenetic analysis of SDR enzymes reveals that 11β-HSD2 and 17β-HSD2 share 36% identical sequences.[21] Therefore, we included 17β-HSD1 and 17β-HSD2 to further assess the specificity of the selected compounds. Compounds **26** and **30** exerted significant inhibition on 17β-HSD2 and did not reach the criteria of at least 10-fold selectivity to inhibit 11β-HSD1. Some inhibition of 17β-HSD1 and 17β-HSD2 was also observed with **25**, **28**, **29**, and **30**, further supporting the inclusion of additional SDR enzymes to assess the selectivity of 11β-HSD1 inhibitors. Recent studies by Koch et al. suggest that structural similarity rather than primary sequence similarity is the important factor determining whether a given chemical interferes with the activity of a related enzyme.[57,58] Thus, in future investigations, the power to predict the selectivity of potential 11β-HSD1 inhibitors could be improved by including pharmacophore models of the closest structurally related enzymes.

Suitable cell lines with an origin from metabolically relevant tissues and expressing endogenous levels of 11β-HSD1 are currently not available; therefore, we employed intact HEK-293 cells that were cotransfected with human 11β-HSD1 and H6PDH. The coexpression with H6PDH determines the reaction direction of 11β-HSD1 as an oxoreductase in metabolically relevant tissues such as liver, skeletal muscle, and adipose tissue.[44,45,59] The kinetic parameters of **25** and **27** determined in transfected HEK-293 cells, mouse 3T3-L1 adipocytes, and differentiated mouse C2C12 myotubes are comparable, indicating that the transfected HEK-293 cell system represents a useful model that does not require differentiation. Furthermore, it shows that **25** and **27** similarly inhibit human and mouse 11β-HSD1. Significant species-specific differences have been reported for several other 11β-HSD1 inhibitors,[26,36] making a comparison between species more complicated.

Elevated glucocorticoid levels in skeletal muscle are associated with insulin resistance and diabetes[6,8] and play an important role in muscle atrophy.[46] Here, we also demonstrate that mouse C2C12 cells express 11β-HSD1 upon differentiation to myotubes and thus represent a suitable system to investigate the role of glucocorticoid reactivation on metabolic and inflammatory parameters in skeletal muscle cells.

The therapeutic benefit of an 11β-HSD1 inhibitor is a reduced tissue-specific reactivation of glucocorticoids with subsequent blockade of GR-mediated regulation of gene expression. 11β-HSDs, GR, and MR all bind glucocorticoids, thereby recognizing some common structural features of the steroid molecule. Thus, compounds that inhibit 11β-HSD1 may exert direct effects on the receptor(s) by binding and acting as (ant-)agonists. To exclude that a selected compound directly activates the receptors and to verify the 11β-HSD1-dependent effect of the compound on receptor activation, GR- and MR-dependent reporter gene assays are useful tools. Indeed, our results show that **27** binds to both GR and MR and antagonizes receptor activation. The inhibition of 11β-HSD1 clearly predominates over the direct receptor effects with a 6−10-fold preference. The weak GR and MR antagonist effects of **27** might rather enhance its therapeutic potential, since it would reduce **2**-mediated stimulation of

gluconeogenesis in the liver and **2**-dependent activation of MR in the kidneys.

Docking experiments enabled us to rationalize the binding of the newly identified inhibitors. All compounds were positioned well in the active site of the enzyme and were found in a similar orientation as the template compound **4**. Compound **25** is located in the hydrophobic tube formed by Leu171, Tyr177, Leu217, and Leu262. The amide nitrogen atom is involved in hydrogen bonding with the catalytic amino acid residue Tyr183. While the steroidal body of **27** is observed in the same area as the **4** core, no direct hydrogen bond with catalytic residues is established; however, hydrophobic interactions can be observed. The carboxyl group forms a hydrogen bond with the cofactor molecule. Compound **31** also shares the hydrophobic cavity and hydrogen bonds with the backbone amide oxygen of Thr124 as well as the hydrophobic interaction with Tyr183. All inhibitors are located in close vicinity to the essential catalytically active amino acid Tyr183. Thus, competitive binding can be assumed as the mode of action.

Active compounds identified by VS often constitute only lead compounds that undergo subsequent chemical refinement enhancing the drugs potency and optimizing other parameters such as solubility, membrane permeability, or toxicity. Especially, compound **25** would be a promising candidate for further chemical refinement and optimization because of its high activity, extraordinary selectivity (Table 5), good tolerability, small molecular weight, and chemical structure, which offers several possible sites of chemical modification. A possible approach for chemical optimization involves the generation of a virtual sublibrary based on the lead compound(s), e.g., with ilib:diverse software.[60] VS, in silico filtering for compounds with activity on antitargets,[28,61] and docking studies set a focus on promising candidates to synthesize and validate in vitro.

We examined if **25** or similar compounds have been described in the literature before. Compound **25** itself has not been reported, neither its synthesis nor any putative biological activity. A similarity search was conducted within the WDI employing the Tanimoto FCFP-4 similarity descriptor embedded in the Pipeline Pilot program.[62] Only one compound was identified revealing a score of >0.60 (the phosphodiesterase inhibitor ZK-73433). Another similarity search conducted in the SciFinder database[63] (filter settings, only references describing a biological study; Tanimoto score $\geq$ 80) returned no substance. When easening the Tanimoto score to ≥ 70, 14 compounds of interest with reported biological activity were returned from the search, including antiproliferative agents as well as 11β-HSD and 17β-HSD inhibitors.[64−67]

Conclusion

Our results demonstrate that inhibitor-based pharmacophore modeling combined with VS of molecule three-dimensional databases can be applied to identify novel classes of 11β-HSD1 inhibitors. Using an 11β-HSD1 selective and a nonselective pharmacophore model, we identified compounds with structures resembling that of the known inhibitor GA and with a sterol/steroidlike structure as well as compounds with structures that have not before been reported as 11β-HSD1 inhibitors. Our results emphasize that for the identification of specific 11β-HSD1 inhibitors, suitable assays including related SDR enzymes have to be performed due to the structural similarity of members of the SDR family of enzymes. Using **27**, we demonstrate efficient and selective inhibition of 11β-HSD1 that result in a subsequent decrease in GR-mediated gene expression. Here, we also introduce the use of differentiated mouse C2C12 myotubes as a suitable endogenous cell system that can be applied in addition to mouse 3T3-L1 adipocytes to study effects on 11β-HSD1 function. Compounds identified by pharmacophore modeling and VS and analyzed in suitable cell-based assays can then be subjected to further chemical and biological optimization for potential therapeutic applications.

Experimental Section

Pharmacophore Model Generation Employing Catalyst. The computational molecular modeling studies were carried out using a Silicon Graphics Octane R12000 workstation running IRIX 6.5.10. A ligand-based approach was used to identify common features of 11β-HSD1 and 11β-HSD2 inhibitors. As a basis for the molecular modeling studies, substances with known activity on 11β-HDS enzymes were extracted from recent literature.[26,36−39,41] The compounds of the training and test set were submitted to energy minimization and conformational analysis (max number of conformers = 250; generation type, best quality; energy range = 20 kcal/mol of minimum) employing the ConFirm program implemented into Catalyst.[68] Using the HipHop algorithm of Catalyst,[69,70] pharmacophore models for highly active 11β-HSD inhibitors were built. For each training set, 10 hypotheses were returned by the hypothesis generation process. The pharmacophore features considered for the models were HBA, HBD, and H features. These features were chosen after a careful analysis of chemical features present in known 11β-HSD inhibitors. After assessing all 10 hypotheses, a search in our in-house database consisting of 11β-HSD inhibitors derived from literature was performed in Best Flexible Search mode[71] to determine which hypothesis could correctly identify potent 11β-HSD inhibitors.

By using the Shape algorithm of Catalyst,[71] spatial information of highly active compounds can be converted into a model. A shape excludes compounds that do not fit in the same space as the template molecule(s) and helps to reduce abundant hitlists derived from database mining.

A search in our in-house DB (the so-called stockroom-DB, Supporting Information Table S-1) of known 11β-HSD inhibitors was conducted with all pharmacophore models as a hypothesis validation step. This DB consists of 114 compounds with known 11β-HSD inhibition properties. All training and test set compounds are derived from the stockroom DB, which consisted of 144 compounds with known activity on either 11β-HSD1 or 11β-HSD2 or both.[26,36,37,39]

MTT Cytotoxicity Assay. HEK-293 cells were grown in poly-D-lysine-coated 96 well plates to avoid cell detachment. Cells were incubated for 4 h at 37 °C with 40 μM of the corresponding chemical, followed by a change to fresh medium containing 0.5 mg/mL of 3-(4,5-dimethylthiazol-2-yl)-2,5-diphenyltetrazolium bromide (MTT). After conversion of MTT ($OD_{A_{570}} - A_{690}$ was kept below 0.9), the medium was removed and 200 μL of DMSO was added to the insoluble fraction. Chloroform (1%, v/v) and sodium hydroxide (50 mM) served as controls.

Activity Assays with Human Recombinant 11β-HSDs and 17β-HSDs in Cell Lysates. Recombinant human 11β-HSDs and 17β-HSDs were expressed in HEK-293 cells that are devoid of endogenous expression of these enzymes, and activities were determined as described previously.[44,47] The 11β-HSD1-dependent oxoreduction of **1** to **2** was determined by using [1,2,6,7-^{3}H]-labeled **1** at a final concentration of 200 nM and 500 μM NADPH. The 11β-HSD2-dependent oxidation of **2** to **1** was measured similarly using radiolabeled **2** (50 nM) and $NADP^+$ (500 μM). The 17β-HSD1-dependent oxoreduction of estrone and the 17β-HSD2-dependent oxidation of estradiol were measured using 200 nM of radiolabeled estrone or estradiol and 500 μM of NADPH and $NADP^+$, respectively. Inhibitors at a final concentration of 50 nM to 30 μM were diluted from stock solutions in DMSO and immediately used for activity assays. The DMSO concentration did not exceed 0.1% and had no effect on enzyme activities. IC_{50} values were calculated using the Data Analysis Toolbox (MDL Information

Systems Inc.) assuming first-order rate kinetics. Data (means ± SD) were obtained from at least four independent experiments.

Activity Assays with Human Recombinant 11β-HSD1 and 11β-HSD2 in Intact Cells. HEK-293 cells were grown in 10 cm dishes in Dulbecco's modified Eagle's medium (DMEM) supplemented with 10% fetal calf serum (FCS) and transfected according to the calcium phosphate precipitation method with an 11β-HSD2 expression plasmid (15 μg) or cotransfected with expression plasmids for 11β-HSD1 and H6PDH (8 μg each). Six hours post-transfection, cells were washed twice with charcoal-stripped medium to remove steroids, detached, and distributed to 96 well plates (30000 cells per well), followed by incubation in steroid-free DMEM for another 18 h. Inhibitors were diluted in steroid-free medium from stock solutions and added at a final concentration between 50 nM and 20 μM, followed by addition of 200 nM radiolabeled **1** or **2**. Incubation for 11β-HSD1-dependent oxoreduction of **1** was 90 min, and for 11β-HSD2-dependent oxidation of **2**, it was 30 min at 37 °C. Reactions were stopped by adding an excess of unlabeled **1** and **2** in methanol, followed by separation of steroids on TLC plates and determination of the conversion of radiolabeled substrate by scintillation counting. Data (means ± SD) were obtained from at least four independent experiments.

11β-HSD1 Activity Assay in Intact Mouse C2C12 Myotubes. C2C12 myocytes were cultured in six well plates containing 2 mL per well of DMEM supplemented with 10% FCS and allowed to achieve confluence (24 h). Myoblasts were then incubated in DMEM supplemented with 2% horse serum for 7 days to induce differentiation into myotubes. At day 7, 11β-HSD1-dependent conversion of 200 nM radiolabeled **1** to **2** in the presence of various concentrations of inhibitors was determined by incubating myotubes for 1 h at 37 °C. A linear increase in the formation of **2** was observed when cells were incubated between 15 and 60 min, with approximately 30% conversion after 60 min. Reactions were stopped, and the conversion of **1** to **2** was assessed by ethyl acetate extraction of steroids from the medium, followed by evaporation of the solvent and separation of steroids by TLC and subsequent scintillation counting.

11β-HSD1 Activity Assay in Intact Mouse 3T3-L1 Adipocytes. 3T3-L1 preadipocytes were cultured in six well plates containing 2 mL of DMEM supplemented with 10% FCS until confluence was achieved, incubated for another 48 h in the same medium, and incubated in differentiation medium (DMEM, 10% FCS, 0.25 mM 3-isobuthyl-1-methylxanthine, 0.5 μM dexamethasone, 1 μg/mL insulin) for another 48 h. The medium was then replaced with adipocyte growth medium (DMEM, 10% FCS, 1 μg/mL insulin) and 72 h later with DMEM and 10% FCS without insulin. 11β-HSD1-dependent conversion of 200 nM radiolabeled **1** to **2** in the presence of various concentrations of inhibitor was determined after incubation of differentiated 3T3-L1 adipocytes for 45 min at 37 °C, followed by extraction of steroids from the medium and determination of the conversion by TLC and scintillation counting.

GR- and MR-Dependent Transactivation Assay. HEK-293 cells were distributed to poly-L-lysine-coated 12 well plates. Each well contained 200000 cells in 1 mL of DMEM and 10% FCS. After 18 h, cells were transfected with 300 ng of pMMTV-LacZ reporter plasmid, 100 ng of pCMV-LUC control plasmid, 150 ng of GR or MR expression vector, and either 150 ng of expression plasmids for 11β-HSD1 and H6PDH or 300 ng of empty pcDNA3 vector. Six hours later, cells were washed twice with steroid-free medium, followed by incubation for another 24 h in the presence of steroid hormone (1 nM aldosterone for MR, 100 nM **2** for GR, and 250 nM **1** for GR with 11β-HSD1 and H6PDH), receptor antagonist (10 μM spironolactone for MR and 10 μM RU486 for GR) or various concentrations of **25** or **27**, respectively. Cells were lysed in 50 μL of lysis buffer, and lysates were analyzed with the luciferase assay system (Promega) and the β-galactosidase galactolight plus kit (Tropix). The galactosidase activity was normalized to the internal luciferase control. Data (means ± SD) were expressed as percentage relative to the control in the presence of steroid but absence of inhibitor and were obtained from four independent experiments.

Docking of Compounds into the 11β-HSD1 Active Site. For the docking experiments, we used GOLD 3.0 software (www.ccdc.cam.ac.uk/products/life_sciences/gold/). GOLD employs a genetic algorithm for finding accurate docking solutions. Furthermore, the program allows full ligand flexibility and partial protein flexibility during docking. Overall, the default parameters of the program were employed. Both protein and ligand atom types were determined by GOLD. Additionally, cocrystallized water molecules were included in the docking process. GOLD 3.0 allows the user to set water molecules within the binding pocket to "toggle", which lets the program decide whether the water should be present or absent (i.e., displaced by the ligand) during docking. Moreover, with the "spin" option, GOLD can automatically optimize the orientation of the hydrogen atoms.[72] However, there is no way to set "toggle" and "spin" as the default options for all water atoms within the binding pocket, thus the user has to enter the atom numbers of the oxygen atoms for each water molecule manually. To circumvent this, we wrote a Perl script, which does the following: (i) take a protein file in mol2 format and a GOLD configuration file and (ii) add all of the water molecules from the protein file to the new GOLD configuration file and sets them to "toggle" and "spin", removing all previous water data from the configuration file. Because GOLD only looks at water molecules within the binding pockets, changing the settings for all of the other water molecules in the protein does not affect the docking run. With this modified configuration file, the following docking experiments were performed. First, the cocrystallized ligand **4** was docked into the LBD to determine whether GOLD could restore the original binding conformation and orientation (Supporting Information, Figure S1). The high consensus of the docked vs the observed binding mode confirmed that our docking protocol was suitable for this target. Accordingly, **25**, **27**, and **31** were docked following this newly established protocol.

Acknowledgment. We thank Dr. Stefan Andersson, University of Texas Southwestern Medical Center, Dallas, for the gift of 17β-HSD1 and 17β-HSD2 expression plasmids and Heidi Jamin for excellent technical support. Dr. Rémy Hoffmann (Accelrys) is thanked for performing the database searches in the WDI. This work was supported by grants from the Cloëtta Research Foundation (A.O.), the Swiss National Science Foundation (Grant 310000-112279 to A.O.), and the Swiss Foundation for Research on Muscle Diseases (A.O.). BioNetWorks GmbH is gratefully acknowledged for financial support.

Supporting Information Available: The full stockroom database compounds (Table S-1) and the supporting Figure S-1 showing **4** docked into the 11β-HSD1 ligand binding site. This material is available free of charge via the Internet at http://pubs.acs.org.

References

(1) Sapolsky, R. M.; Romero, L. M.; Munck, A. U. How do glucocorticoids influence stress responses? Integrating permissive, suppressive, stimulatory, and preparative actions. *Endocr. Rev.* **2000**, *21*, 55−89.
(2) Charmandari, E.; Kino, T.; Chrousos, G. P. Glucocorticoids and their actions: an introduction. *Ann. N. Y. Acad. Sci.* **2004**, *1024*, 1−8.
(3) Ishida-Takahashi, R.; Uotani, S.; Abe, T.; Degawa-Yamauchi, M.; Fukushima, T.; et al. Rapid inhibition of leptin signaling by glucocorticoids in vitro and in vivo. *J. Biol. Chem.* **2004**, *279*, 19658−19664.
(4) Lambillotte, C.; Gilon, P.; Henquin, J. C. Direct glucocorticoid inhibition of insulin secretion. An in vitro study of dexamethasone effects in mouse islets. *J. Clin. Invest.* **1997**, *99*, 414−423.
(5) Dimitriadis, G.; Leighton, B.; Parry-Billings, M.; Sasson, S.; Young, M.; et al. Effects of glucocorticoid excess on the sensitivity of glucose transport and metabolism to insulin in rat skeletal muscle. *Biochem. J.* **1997**, *321* (Part 3), 707−712.
(6) Abdallah, B. M.; Beck-Nielsen, H.; Gaster, M. Increased expression of 11beta-hydroxysteroid dehydrogenase type 1 in type 2 diabetic myotubes. *Eur. J. Clin. Invest.* **2005**, *35*, 627−634.
(7) Lundgren, M.; Buren, J.; Ruge, T.; Myrnas, T.; Eriksson, J. W. Glucocorticoids down-regulate glucose uptake capacity and insulin-signaling proteins in omental but not subcutaneous human adipocytes. *J. Clin. Endocrinol. Metab.* **2004**, *89*, 2989−2997.

(8) Whorwood, C. B.; Donovan, S. J.; Flanagan, D.; Phillips, D. I.; Byrne, C. D. Increased glucocorticoid receptor expression in human skeletal muscle cells may contribute to the pathogenesis of the metabolic syndrome. *Diabetes* **2002**, *51*, 1066−1075.
(9) Odermatt, A. 11beta-hydroxysteroid dehydrogenase type 1: A potential therapeutic target for the control of local glucocorticoid concentrations. *Curr. Enzyme Inhib.* **2005**, *1*, 97−105.
(10) Masuzaki, H.; Paterson, J.; Shinyama, H.; Morton, N. M.; Mullins, J. J.; et al. A transgenic model of visceral obesity and the metabolic syndrome. *Science* **2001**, *294*, 2166−2170.
(11) Masuzaki, H.; Yamamoto, H.; Kenyon, C. J.; Elmquist, J. K.; Morton, N. M.; et al. Transgenic amplification of glucocorticoid action in adipose tissue causes high blood pressure in mice. *J. Clin. Invest.* **2003**, *112*, 83−90.
(12) Paterson, J. M.; Morton, N. M.; Fievet, C.; Kenyon, C. J.; Holmes, M. C.; et al. Metabolic syndrome without obesity: Hepatic overexpression of 11beta-hydroxysteroid dehydrogenase type 1 in transgenic mice. *Proc. Natl. Acad. Sci. U.S.A.* **2004**, *101*, 7088−7093.
(13) Kotelevtsev, Y.; Holmes, M. C.; Burchell, A.; Houston, P. M.; Schmoll, D.; et al. 11beta-hydroxysteroid dehydrogenase type 1 knockout mice show attenuated glucocorticoid-inducible responses and resist hyperglycemia on obesity or stress. *Proc. Natl. Acad. Sci. U.S.A.* **1997**, *94*, 14924−14929.
(14) Lindsay, R. S.; Wake, D. J.; Nair, S.; Bunt, J.; Livingstone, D. E.; et al. Subcutaneous adipose 11 beta-hydroxysteroid dehydrogenase type 1 activity and messenger ribonucleic acid levels are associated with adiposity and insulinemia in Pima Indians and Caucasians. *J. Clin. Endocrinol. Metab.* **2003**, *88*, 2738−2744.
(15) Valsamakis, G.; Anwar, A.; Tomlinson, J. W.; Shackleton, C. H.; McTernan, P. G.; et al. 11beta-hydroxysteroid dehydrogenase type 1 activity in lean and obese males with type 2 diabetes mellitus. *J. Clin. Endocrinol. Metab.* **2004**, *89*, 4755−4761.
(16) Rask, E.; Walker, B. R.; Soderberg, S.; Livingstone, D. E.; Eliasson, M.; et al. Tissue-specific changes in peripheral cortisol metabolism in obese women: Increased adipose 11beta-hydroxysteroid dehydrogenase type 1 activity. *J. Clin. Endocrinol. Metab.* **2002**, *87*, 3330−3336.
(17) Paulmyer-Lacroix, O.; Boullu, S.; Oliver, C.; Alessi, M. C.; Grino, M. Expression of the mRNA coding for 11beta-hydroxysteroid dehydrogenase type 1 in adipose tissue from obese patients: An in situ hybridization study. *J. Clin. Endocrinol. Metab.* **2002**, *87*, 2701−2705.
(18) Kannisto, K.; Pietilainen, K. H.; Ehrenborg, E.; Rissanen, A.; Kaprio, J.; et al. Overexpression of 11beta-hydroxysteroid dehydrogenase-1 in adipose tissue is associated with acquired obesity and features of insulin resistance: Studies in young adult monozygotic twins. *J. Clin. Endocrinol. Metab.* **2004**, *89*, 4414−4421.
(19) Frey, F. J.; Odermatt, A.; Frey, B. M. Glucocorticoid-mediated mineralocorticoid receptor activation and hypertension. *Curr. Opin. Nephrol. Hypertens.* **2004**, *13*, 451−458.
(20) Odermatt, A.; Arnold, P.; Stauffer, A.; Frey, B. M.; Frey, F. J. The N-terminal anchor sequences of 11beta-hydroxysteroid dehydrogenases determine their orientation in the endoplasmic reticulum membrane. *J. Biol. Chem.* **1999**, *274*, 28762−28770.
(21) Baker, M. E. Evolutionary analysis of 11beta-hydroxysteroid dehydrogenase-type 1, -type 2, -type 3 and 17beta-hydroxysteroid dehydrogenase-type 2 in fish. *FEBS Lett.* **2004**, *574*, 167−170.
(22) Hosfield, D. J.; Wu, Y.; Skene, R. J.; Hilgers, M.; Jennings, A.; et al. Conformational flexibility in crystal structures of human 11beta-hydroxysteroid dehydrogenase type I provide insights into glucocorticoid interconversion and enzyme regulation. *J. Biol. Chem.* **2005**, *280*, 4639−4648.
(23) Ogg, D.; Elleby, B.; Norstroem, C.; Stefansson, K.; Abrahmsen, L.; et al. The crystal structure of guinea pig 11b-hydroxysteroid dehydrogenase type 1 provides a model for enzyme-lipid bilayer interactions. *J. Biol. Chem.* **2005**, *280*, 3789−3794.
(24) Zhang, J.; Osslund, T. D.; Plant, M. H.; Clogston, C. L.; Nybo, R. E.; et al. Crystal structure of murine 11β-hydroxysteroid dehydrogenase 1: An important therapeutic target for diabetes. *Biochemistry* **2005**, *44*, 6948−6957.
(25) Berman, H. M.; Westbrook, J.; Feng, Z.; Gilliland, G.; Bhat, T. N.; et al. The protein data bank. *Nucleic Acids Res.* **2000**, *28*, 235−242.
(26) Arampatzis, S.; Kadereit, B.; Schuster, D.; Balazs, Z.; Schweizer, R. A.; et al. Comparative enzymology of 11beta-hydroxysteroid dehydrogenase type 1 from six species. *J. Mol. Endocrinol.* **2005**, *35*, 89−101.
(27) Jorgensen, W. L. The many roles of computation in drug discovery. *Science* **2004**, *303*, 1813−1818.
(28) Ekins, S. Predicting undesirable drug interactions with promiscuous proteins in silico. *Drug Discovery Today* **2004**, *9*, 276−285.
(29) Kurogi, Y.; Guner, O. F. Pharmacophore modeling and three-dimensional database searching for drug design using catalyst. *Curr. Med. Chem.* **2001**, *8*, 1035−1055.
(30) Bajorath, J. Integration of virtual and high-throughput screening. *Nat. Rev. Drug Discovery* **2002**, *1*, 882−894.
(31) Shoichet, B. K. Virtual screening of chemical libraries. *Nature* **2004**, *432*, 862−865.
(32) van de Waterbeemd, H.; Gifford, E. ADMET in silico modelling: towards prediction paradise? *Nat. Rev. Drug Discovery* **2003**, *2*, 192−204.
(33) Lipinski, C. A.; Lombardo, F.; Dominy, B. W.; Feeney, P. J. Experimental and computational approaches to estimate solubility and permeability in drug discovery and development settings. *Adv. Drug Delivery Rev.* **1997**, *23*, 3−25.
(34) Lipinski, C. A. Lead- and drug-like compounds: The rule-of-five revolution. *Drug Discovery Today* **2004**, *1*, 337−341.
(35) Doman, T. N.; McGovern, S. L.; Witherbee, B. J.; Kasten, T. P.; Kurumbail, R.; et al. Molecular docking and high-throughput screening for novel inhibitors of protein tyrosine phosphatase-1B. *J. Med. Chem.* **2002**, *45*, 2213−2221.
(36) Barf, T.; Vallgarda, J.; Emond, R.; Haggstrom, C.; Kurz, G.; et al. Arylsulfonamidothiazoles as a new class of potential antidiabetic drugs. Discovery of potent and selective inhibitors of the 11β-hydroxysteroid dehydrogenase type 1. *J. Med. Chem.* **2002**, *45*, 3813−3815.
(37) Vicker, N.; Su, X.; Ganeshapillai, D.; Purohit, A.; Reed, M. J.; et al. Inhibitors of 11-beta-hydroxy steroid dehydrogenase type 1 and type 2. WO 2004/037251.
(38) Morris, D. J.; Souness, G. W.; Latif, S. A.; Hardy, M. P.; Brem, A. S. Effect of chenodeoxycholic acid on 11b-hydroxysteroid dehydrogenase in various target tissues. *Metab. Clin. Exp.* **2004**, *53*, 811−816.
(39) Stauffer, A. T.; Rochat, M. K.; Dick, B.; Frey, F. J.; Odermatt, A. Chenodeoxycholic acid and deoxycholic acid inhibit 11 beta-hydroxysteroid dehydrogenase type 2 and cause cortisol-induced transcriptional activation of the mineralocorticoid receptor. *J. Biol. Chem.* **2002**, *277*, 26286−26292.
(40) *Derwent World Drug Index*, 2003 ed.; Derwent Publications Ltd.: London, 2003.
(41) Vicker, N.; Su, X.; Lawrence, H.; Cruttenden, A.; Purohit, A.; et al. A novel 18beta-glycyrrhetinic acid analogue as a potent and selective inhibitor of 11beta-hydroxysteroid dehydrogenase 2. *Bioorg. Med. Chem. Lett.* **2004**, *14*, 3263−3267.
(42) Schuster, D.; Laggner, C.; Steindl, T. M.; Palusczak, A.; Hartmann, R. W.; Langer, T. Pharmacophore modeling and in silico screening for new P450 19 (aromatase) inhibitors. *J. Comput. Inf. Model.* **2006**, ASAP Article; DOI: 10.1021/ci050237k.
(43) Niederreiter, D. *Why Drugs Fail—A Study on Side Effects in New Chemical Entities*; Department of Pharmaceutical Chemistry, University of Innsbruck: Innsbruck, 2004.
(44) Atanasov, A. G.; Nashev, L. G.; Schweizer, R. A.; Frick, C.; Odermatt, A. Hexose-6-phosphate dehydrogenase determines the reaction direction of 11beta-hydroxysteroid dehydrogenase type 1 as an oxoreductase. *FEBS Lett.* **2004**, *571*, 129−133.
(45) Lavery, G. G.; Walker, E. A.; Draper, N.; Jeyasuria, P.; Marcos, J.; et al. Hexose-6-phosphate dehydrogenase knockout mice lack 11beta-hydroxysteroid dehydrogenase type 1-mediated glucocorticoid generation. *J. Biol. Chem.* **2006**, *281*, 6546−6551.
(46) Hasselgren, P. O. Glucocorticoids and muscle catabolism. *Curr. Opin. Clin. Nutr. Metab. Care* **1999**, *2*, 201−205.
(47) Schweizer, R. A.; Atanasov, A. G.; Frey, B. M.; Odermatt, A. A rapid screening assay for inhibitors of 11beta-hydroxysteroid dehydrogenases (11beta-HSD): Flavanone selectively inhibits 11beta-HSD1 reductase activity. *Mol. Cell. Endocrinol.* **2003**, *212*, 41−49.
(48) Sandeep, T. C.; Yau, J. L.; MacLullich, A. M.; Noble, J.; Deary, I. J.; et al. 11Beta-hydroxysteroid dehydrogenase inhibition improves cognitive function in healthy elderly men and type 2 diabetics. *Proc. Natl. Acad. Sci. U.S.A.* **2004**, *101*, 6734−6739.
(49) Small, G. R.; Hadoke, P. W.; Sharif, I.; Dover, A. R.; Armour, D.; et al. Preventing local regeneration of glucocorticoids by 11beta-hydroxysteroid dehydrogenase type 1 enhances angiogenesis. *Proc. Natl. Acad. Sci. U.S.A.* **2005**, *102*, 12165−12170.
(50) Alberts, P.; Nilsson, C.; Selen, G.; Engblom, L. O.; Edling, N. H.; et al. Selective inhibition of 11 beta-hydroxysteroid dehydrogenase type 1 improves hepatic insulin sensitivity in hyperglycemic mice strains. *Endocrinology* **2003**, *144*, 4755−4762.
(51) Alberts, P.; Engblom, L.; Edling, N.; Forsgren, M.; Klingstrom, G.; et al. Selective inhibition of 11beta-hydroxysteroid dehydrogenase type 1 decreases blood glucose concentrations in hyperglycaemic mice. *Diabetologia* **2002**, *45*, 1528−1532.
(52) Hermanowski-Vosatka, A.; Balkovec, J. M.; Cheng, K.; Chen, H. Y.; Hernandez, M.; et al. 11beta-HSD1 inhibition ameliorates metabolic syndrome and prevents progression of atherosclerosis in mice. *J. Exp. Med.* **2005**, *202*, 517−527.

(53) Coppola, G. M.; Kukkola, P. J.; Stanton, J. L.; Neubert, A. D.; Marcopulos, N.; et al. Perhydroquinolylbenzamides as novel inhibitors of 11β-hydroxysteroid dehydrogenase type 1. *J. Med. Chem.* **2005**, *48*, 6696−6712.
(54) Fotsch, C.; Askew, B. C.; Chen, J. J. 11beta-Hydroxysteroid dehydrogenase-1 as a therapeutic target for metabolic diseases. *Expert Opin. Ther. Pat.* **2005**, *15*, 289−303.
(55) Su, X.; Lawrence, H.; Ganeshapillai, D.; Cruttenden, A.; Purohit, A.; et al. Novel 18beta-glycyrrhetinic acid analogues as potent and selective inhibitors of 11beta-hydroxysteroid dehydrogenases. *Bioorg. Med. Chem.* **2004**, *12*, 4439−4457.
(56) Odermatt, A.; Atanasov, A. G.; Balazs, Z.; Schweizer, R. A.; Nashev, L. G.; et al. Why is 11beta-hydroxysteroid dehydrogenase type 1 facing the endoplasmic reticulum lumen? Physiological relevance of the membrane topology of 11beta-HSD1. *Mol. Cell. Endocrinol.* **2006**, *248*, 15−30.
(57) Koch, M. A.; Wittenberg, L. O.; Basu, S.; Jeyaraj, D. A.; Gourzoulidou, E.; et al. Compound library development guided by protein structure similarity clustering and natural product structure. *Proc. Natl. Acad. Sci. U.S.A.* **2004**, *101*, 16721−16726.
(58) Koch, M. A.; Schuffenhauer, A.; Scheck, M.; Wetzel, S.; Casaulta, M.; et al. Charting biologically relevant chemical space: a structural classification of natural products (SCONP). *Proc. Natl. Acad. Sci. U.S.A.* **2005**, *102*, 17272−17277.
(59) Bujalska, I. J.; Walker, E. A.; Hewison, M.; Stewart, P. M. A switch in dehydrogenase to reductase activity of 11beta-hydroxysteroid dehydrogenase type 1 upon differentiation of human omental adipose stromal cells. *J. Clin. Endocrinol. Metab.* **2002**, *87*, 1205−1210.
(60) Langer, T.; Wolber, G. Virtual combinatorial chemistry and in silico screening: Efficient tools for lead structure discovery? *Pure Appl. Chem.* **2004**, *76*, 991−996.
(61) Recanatini, M.; Bottegoni, G.; Cavalli, A. In silico antitarget screening. *Drug Discovery Today* **2004**, *1*, 209−215.
(62) *Pipeline Pilot*, Vers. 5.0.1.100; SciTegic: San Diego, CA, 2005.
(63) *SciFinder*, 2006 ed.; American Chemical Society: Washington, DC, 2006.
(64) Reddy, N. L.; Hill, J.; Ye, L.; Fernandes, P. B.; Stout, D. M. Identification and strucutreactivity relationship studies of 3-methylene-2-norbornanone as potent anti-proliferative agents presumably working through p53 mediated apoptosis. *Bioorg. Med. Chem.* **2004**, *14*, 5645−5649.
(65) Natarajan, S. K.; Moreno, O.; Graddis, T. J.; Duncan, D.; Laus, R.; et al. Compositions and methods for the treatment for disease associated with Trp-p8 expression. WO 2005/020897, March 10, 2005.
(66) Andersen, H. S.; T., K. G. C.; Christensen, I. T.; Mogensen, J. P.; Larsen, A. R.; et al. Pharmaceutical use of substituted amides. WO 2004/089470, October 21, 2004.
(67) Kampen, G. C. T.; Andersen, H. S. Combination therapy using an 11beta-hydroxysteroid dehydrogenase type 1 inhibitor and a glucocorticoid receptor agonist to minimize the side effects associated with glucocorticoid receptor agonist therapy. WO 2004/089415, October 21, 2004.
(68) *Catalyst Software Package*, Version 4.9; Accelrys Software Inc.: San Diego, CA, 2003.
(69) Barnum, D.; Greene, J.; Smellie, A.; Sprague, P. Identification of common functional configurations among molecules. *J. Chem. Inf. Comput. Sci.* **1996**, *36*, 536−571.
(70) Clement, O. O.; Mehl, A. T. HipHop: Pharmacophores based on multiple common-feature alignments. *Pharmacophore Perception, Development, and Use in Drug Design*; International University Line: La Jolla, CA, 2000; pp 69−84.
(71) *Catalyst Software Package*, Tutorial Release 4.9; Accelrys Software Inc.: San Diego, CA, 2003.
(72) Verdonk, M. L.; Chessari, G.; Cole, J. C.; Hartshorn, M. J.; Murray, C. W.; et al. Modeling water molecules in protein−ligand docking using GOLD. *J. Med. Chem.* **2005**, *48*, 6504−6515.

JM0600794